Embedding NbN nanowires into quantum circuits with a neon focused ion beam

J. Burnett, J. Sagar, P. A. Warburton and J. C. Fenton

***Abstract*—Parasitic two-level systems are generally present in superconducting circuits as a result of conventional fabrication and processing, and these lead to noise and loss of coherence in quantum systems. We examine the use of a Ne focused ion beam for producing nanowires integrated into superconducting circuits with a minimised density of parasitic two-level systems. We report measurements of nanowires produced by Ne focused-ion-beam milling in NbN resonators. The resonator losses increase after the nanowire is fabricated, with the Q factor decreasing by $\sim 30\%$ to $\sim 10^5$, which is a factor 10–100 higher than in the most closely comparable circuits previously measured. This indicates that the Ne focused ion beam is a promising route for creating superconducting-nanowire-based devices with low levels of decoherence.**

I. Introduction

Superconducting nanowires, in which two dimensions of the superconductor are approximately the same as the superconducting coherence length, have been used to demonstrate a variety of quantum effects. In conventional superconductors such as niobium or aluminium they can constitute Josephson-type weak links [1], [2], whereas in superconductors with a high normal-state resistance, the large kinetic inductance means that these constrictions can act as quantum phase-slip junctions [3], [4]. Devices based upon superconducting nanowires are currently in their infancy and the specifics of how best to integrate these nanowires into quantum circuits is relatively unexplored, even though these details are of crucial importance for any device based upon a coherent quantum process. Superconducting resonators have become the common circuit for the interrogation of coherent quantum devices. The superconducting resonator itself has been very well studied, with recent results showing these resonators to be suitable for quantifying the effects [5] of parasitic two level systems (TLS). These TLS are responsible for high levels of decoherence in superconducting circuits and are now understood to arise in amorphous dielectrics such as resist residues, surface oxides and the interfaces between different materials. While state-of-the-art superconducting resonators can demonstrate an internal quality factor in excess of 10^6 in the single photon limit [6], this value falls when a quantum element is introduced to the resonator, associated with the introduction of additional TLS into the circuit environment due to the additional fabrication. Resonators with conventional Josephson elements routinely demonstrate internal quality factors approaching 10^5 [7]. Considering that conventional Josephson junctions require extra material deposition and oxidation in a lift-off process which uses additional resist coating, it is surprising that such processing is possible with such a low level of additional TLS.

Conversely, the superconducting nanowire can be realised without additional material deposition and in some instances [8], [9] without an additional resist coating. In principle this should allow superconducting nanowires to act as quantum elements without the introduction of excess TLS. Superconducting nanowires have been introduced into a resonator by means of two-angle evaporation [1], Ga focused ion beam [9], carbon nanotube scaffold [8] and with HSQ resist [3], [10]. These methods have enabled the demonstration of magnetic-field-tuneable resonators [1], [8] and coherent quantum phase-slip [3], [10]. However, in all these cases the internal quality factor of the nanowire-embedded resonator has been <5000, considerably lower than state-of-the-art Josephson-junction-based devices, suggesting nanowire devices have yet to be optimised for low-loss characteristics.

In this paper we explore the use of a Ne focused ion beam (FIB) to directly mill nanowires into superconducting resonators. Inert-gas ion beams have become commercially available following the development of the Gas Field Ion Source (GFIS). The GFIS comprises a metallic tip, typically tungsten, which is structured in-situ to become terminated by a trimer of atoms. When held at high voltage, typically 25–35 kV, this atomically defined tip becomes the source of ionisation for the gas in the surrounding environment; He or Ne may be used [11]. Using the resulting beam of noble-gas ions it is possible to achieve a probe size, and as a result imaging resolution, of 0.5 nm for He [12] and 1.9 nm for Ne [11]. The significant mass of the ions can be utilised to remove irradiated material whilst their inert nature is expected to avoid the destructive beam-ion intermixing which arises with Ga ion beams [13].

Superconducting resonators are very sensitive probes of their electromagnetic environment; changes in this environment shift the resonant frequency, and these allow the use of superconducting resonators to study surrounding dielectrics [14], [5] and the effect of implanted magnetic ions [15], therefore superconducting resonators are suitable devices to make comparative measurements before and after nanowires are embedded via a Ne FIB. Such comparative measurements can reveal the degree of loss associated with the fabrication

The authors are with the London Centre for Nanotechnology, University College London, London WC1H 0AH, United Kingdom (email: jonathan.burnett@ucl.ac.uk).

J. Burnett & J. C. Fenton were supported by the UK EPSRC grant reference EP/J017329/1. J. Sagar & P. A. Warburton were supported by the UK EPSRC grant reference EP/K024701/1 and Carl Zeiss SMT.

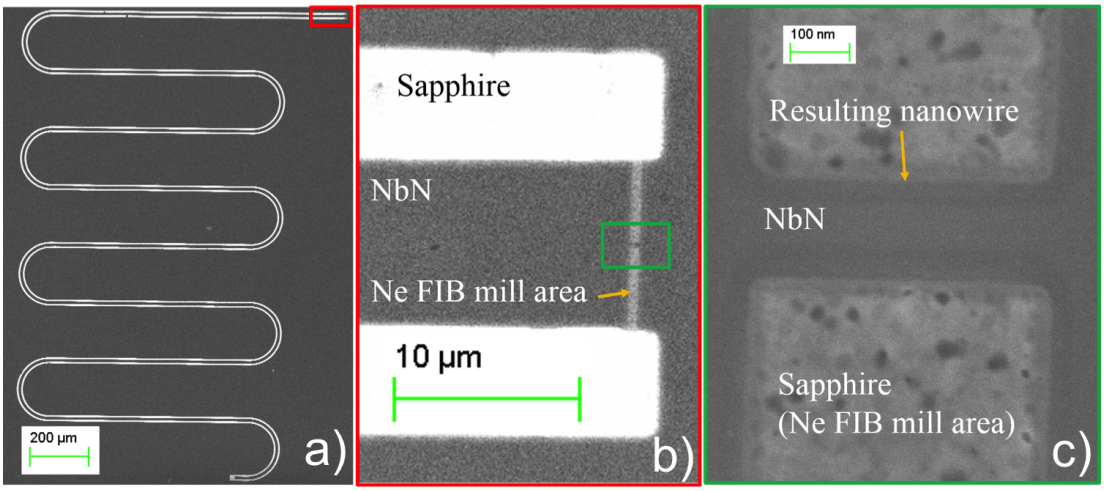

Fig. 1. Scanning electron microscope images of the device Res1. In all images the dark areas are NbN and the light areas are the sapphire substrate. (a) An image of a $\lambda/4$ coplanar resonator. (b) a higher-magnification image of the grounded end of the coplanar resonator (region highlighted by red box in image (a)), the Ne FIB mill area is identified by the light-grey regions. (c) a higher-magnification image of the resulting nanowire after milling by Ne FIB, note the two tones of grey in the nanowire region, the lighter grey area is 100 nm wide and the darker region is 160 nm wide (this region is shown in the green box of image (b)).

of nanowire elements in a resonator.

II. Experimental

NbN resonators are patterned in films deposited on c-axis sapphire substrates. DC magnetron sputtering is used to deposit the NbN from a 99.99%-pure 2" Nb target. The sputtering occurs at room temperature after pumping to 7×10^{-7} mbar; the sputter power is 150 W and the sputter pressure is 5×10^{-3} mbar consisting of equal parts Ar and N_2. The resulting 10-nm-thick NbN film has a superconducting critical temperature T_c of 8 K and sheet resistance $R_\square$ of 700 Ω. These films are patterned into superconducting resonators by forming an etch mask in PMMA using electron beam lithography. A reactive ion etch using SF_6/Ar in a 2:1 ratio at 25 mTorr and 30 W then forms the superconducting resonators. The superconducting resonators consist of coplanar waveguides in a $\lambda/4$ geometry (shown in fig. 1a), with centre frequencies between 3 and 8 GHz. The open end of each resonator forms the coupler, which couples all the resonators to a common microwave feed-line. The coupler has a length of 50 μm and the coupling strength is tuned by varying the distance between the coupler and the feed-line.

A Ne FIB is used to embed nanowires in the central conductor of such superconducting resonators, at the closed end of the resonator, where the current is maximal. Areas to be removed by Ne-FIB are irradiated with a Ne-ion dose of 0.5 nC/μm^2, using Ne ions accelerated to 13 kV and a typical beam current of 2.2 pA.

For characterisation measurements, a ^{3}He refrigerator is used to cool the superconducting resonators to temperatures between 0.35 and 2 K. The resonators are wire-bonded to a microwave PCB which is anchored to the ^{3}He pot. The input microwave line has 40 dB of attenuation between room temperature and the ^{3}He pot. A further 20 dB of attenuation is used at room temperature outside of the ^{3}He refrigerator. The output line has a microwave HEMT amplifier at 7 K (the noise temperature of the amplifier is 2.2 K at this temperature). Between the amplifier and the ^{3}He pot there are two further attenuators with a total attenuation of 9 dB. This level of attenuation is sufficient to reduce thermal photons to a level equivalent to a 200 mK black body. Since this temperature is below that of the ^{3}He pot, we can conclude that thermal photons generated by the sample should be the most energetic photons in the sample. Away from the ^{3}He pot the output microwave line is amplified by another microwave amplifier. A 2 dB attenuator is located between the cryogenic and room-temperature amplifiers to suppress standing waves and there is a 2.7 GHz-high-pass filter after the room-temperature amplifier. The combination of the HEMT bandwidth and the high-pass microwave filter means that the measurement bandwidth is $2.7 - 8.5$ GHz. Microwave measurements are performed using a vector network analyser, which can measure the complex S_{21} response of the superconducting resonators at microwave powers between -50 dBm and -140 dBm.

The complex S_{21} response of the superconducting resonators is a notch which can be fitted by [16]:

$$S_{21}^{\text{notch}}(\nu) = ae^{j\alpha}e^{-2\pi\nu\tau}\left[1 - \frac{(Q_l/|Q_c|)e^{j\phi}}{1 + 2jQ_l(\nu/\nu_0 - 1)}\right], \quad (1)$$

where ν is the frequency of the applied microwave signal and the terms inside the square brackets describe the resonator, with ν_0 being the resonance frequency, Q_l the loaded quality factor and $|Q_c|$ the absolute value of the coupling quality factor; ϕ accounts for any impedance mismatch. The terms outside the square brackets describe the effect of the environment: a describes a change in amplitude, α a change in phase and τ a change in the electronic delay.

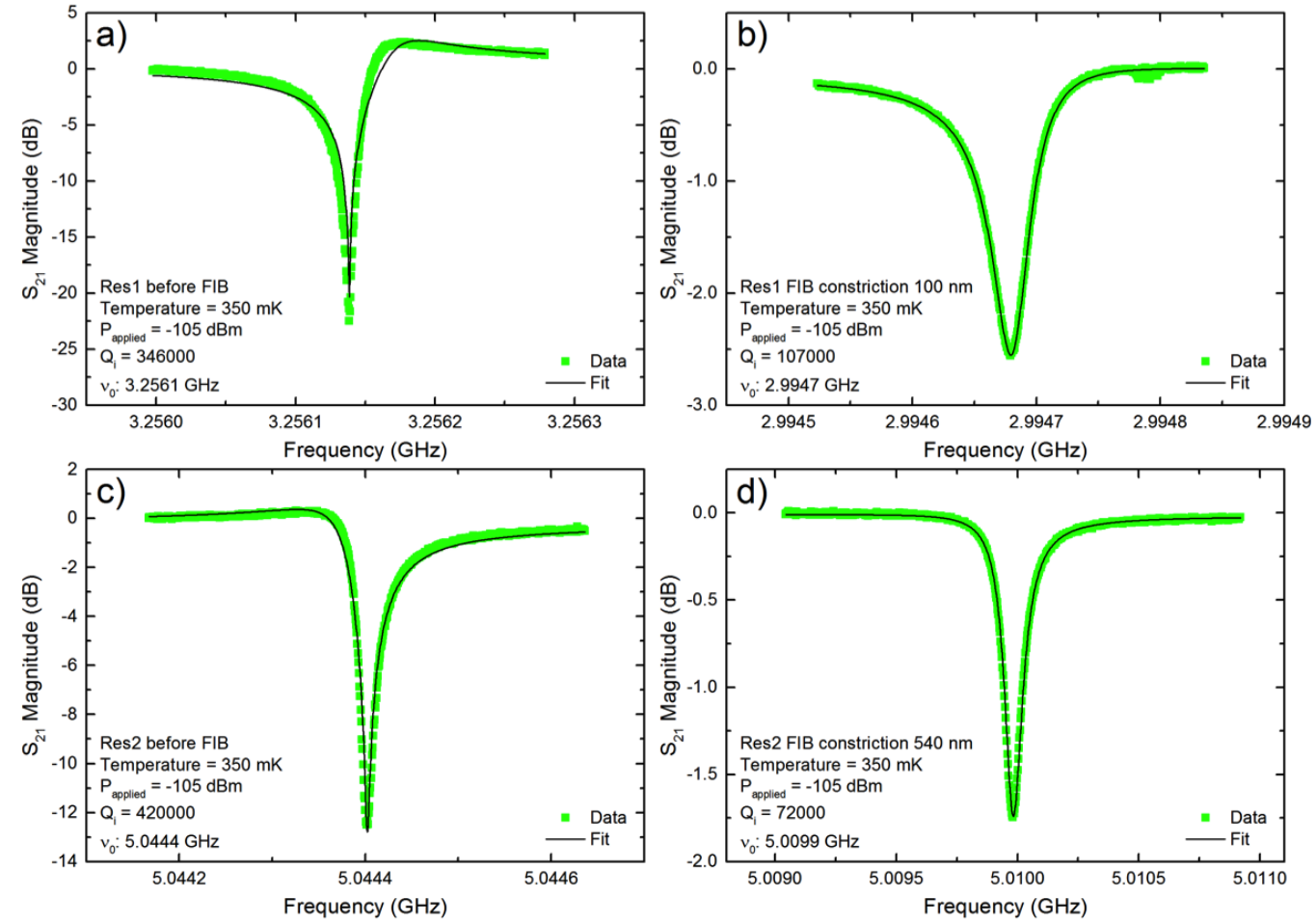

Fig. 2. S_{21} magnitude response at T = 350 mK and P_{applied} = −105 dBm (green points). (a) Res1 before Ne FIB, (b) Res1 after Ne FIB has embedded into it a nanowire with a width of 100 nm, (c) Res2 before Ne FIB, (d) Res2 after a Ne FIB has embedded into it a nanowire with a width of 540 nm. The black lines show fits to equation 1, from which resonator parameters are extracted.

There is also another quality factor, Q_{i}, the internal quality factor, which is related to the other quality factors by $1/Q_{\mathrm{l}} = 1/Q_{\mathrm{c}} + 1/Q_{\mathrm{i}}$. Importantly, a resonator with a notch response allows the accurate determination of both Q_{c} and Q_{i} [16]. In superconducting resonators, Q_{i} is sensitive to the superconducting state for temperatures $T > T_{\mathrm{c}}/10$ [17] and is sensitive to TLS in the low-temperature limit $T \ll T_{\mathrm{c}}$.

We report measurements on two resonators, which we denote Res1 and Res2, with different lengths, patterned on a single chip. The resonators were first measured prior to milling by the Ne FIB. The S_{21} magnitude response of the resonators at 350 mK and a microwave input power −105 dBm is shown in Figs. 2a and c. The response was fitted to equation 1 to determine ν_0 and Q_{i}. Res1 (Res2) had a centre frequency of ν_0 = 3.256 GHz (ν_0 = 5.044 GHz) and Q_{i} = 3.46×10^5 (Q_{i} = 4.2×10^5).

A nanowire was then embedded in the central conductor of the resonator using a Ne FIB. Figure 1 highlights the two mill regions and the resulting nanowire. The scanning electron microscope images allow the dimensions to be determined, for Res2 a width of 540 nm and a length of 500 nm is found. In Fig. 1c the nanowire in Res1 is 350 nm in length, with a central lighter grey region and an outer darker region which received some Ne FIB dose, meaning that the nanowire is likely to have a trapezoidal cross section with a central width of 100 nm and an outer width of 160 nm. The central 100 nm of the nanowire is the same thickness as the rest of the device.

Figures 2b and 2d show measurements of the S_{21} magnitude response of Res1 and Res2 with the embedded nanowire, again at 350 mK and −105 dBm: the new centre frequency for Res1 (Res2) was ν_0 = 2.995 GHz (ν_0 = 5.009 GHz) and Q_{i} = 1.07×10^5 (Q_{i} = 0.72×10^5). The observed resonant frequency has decreased; this is consistent with the introduction of an additional inductance due to the nanowire, since a constriction increases the normal-state resistance and consequently the kinetic inductance. For a $\lambda/4$ resonator the centre frequency is related to the inductance and capacitance per unit length by

$$\nu_0 = \frac{1}{4l\sqrt{L_l C_l}}, \tag{2}$$

where l is the resonator length, L_l the inductance per unit length and C_l the capacitance per unit length, which can be calculated using elliptic integrals[18]. Assuming that the embedding of the nanowire leads to a negligible change in C_l the measured frequency shift can be attributed to an inductance shift which can be calculated using equation 2. Using the resonator lengths of 8.05 mm (5.15 mm) for Res1 (Res2), C_l = 1.48×10^{-10} F/m and the bare resonant frequency of 3.25 GHz (5.044 GHz), the resulting total inductance $L_{\rm tot}$ is found to be 4.95 nH (3.23 nH). After the nanowire is embedded the new centre frequency of 2.995 GHz (5.009 GHz) leads to a new total inductance $L_{\rm tot}$ of 5.85 nH (3.27 nH), corresponding to an additional inductance of 0.9 nH (0.045 nH).

For a superconductor in the dirty limit at T = 0 K, the kinetic inductance can be estimated from[19]

$$L_{\rm K} = 0.18\hbar R_{\rm N}/(k_{\rm B}T_{\rm c}), \tag{3}$$

where $R_{\rm N}$ is the normal state resistance, $\hbar$ is the reduced Planck constant and $k_{\rm B}$ is the Boltzmann constant. Measurements of nanowires patterned in films similar to the one measured here, with the same thickness[20], reveal a normal-state sheet resistance $R_\square$ of ≈ 700 Ω. Using equation 3, the kinetic inductance from the wire with length 500 nm and width 500 nm (Res2) is estimated to be $L_{\rm K}$ = 0.12 nH, whereas assuming the wire in Res1 has length 350 nm and width 100 nm the resulting kinetic inductance should be approximately $L_{\rm K}$ = 0.42 nH. These estimates are within a factor 3 of the inductance inferred from the measured frequency shift. A discrepancy is not unexpected since equation 3 is only valid in the T = 0 K limit, and also the resistance and T_c of the nanowire could be different to that of the film due to damage from the Ne FIB. Another reason to expect a discrepancy between the two values may be because of the contrast between the localised change in the resonator caused by fabricating the nanowire and the assumption of homogeneous change in resonator inductance implicit in extracting the inductance from the resonant frequency; however, a similar assumption is frequently used with bilayer kinetic inductance detectors[21].

The fits to the frequency response show that the internal quality factors decreased by a factor of 10–50 following the Ne FIB milling to create the nanobridges. This is consistent with the focused ion beam leading to an increased density of TLS. Monte Carlo simulations of similar beam parameters to those we used to mill the NbN find a stopping distance in sapphire of ~100 nm [22]. It is therefore expected that doses sufficient to mill the NbN also lead to many ions passing through the film and instead damaging the sapphire substrate, possibly becoming embedded within the top 100 nm of the sapphire. Such damage to the substrate would lead to increased amorphization of the sapphire and consequently increase the density of TLS [23], accounting for the observed decrease in $Q_{\rm i}$ after the use of the Ne FIB.

However, it is also worthwhile to compare the obtained $Q_{\rm i}$ with the $Q_{\rm i}$ obtained for other superconducting resonators embedded with superconducting nanowires or conventional Josephson elements. The $Q_{\rm i}$ = 1×10^5 observed here is a factor of 10–50 higher than previous nanowire-embedded resonators [1], [3], [8] and is comparable to conventional Josephson elements within resonators [7].

We also note that the 100 nm width by no means represents the narrowest nanowire that can be made by this method and preliminary results suggest that 20-nm-wide nanowires should be possible.

III. Conclusion

A neon FIB has been used to create constrictions with a width down to 100 nm in NbN superconducting microwave resonators. This produces a shift in the resonant frequency, as expected due to the kinetic inductance of the nanowire. The internal quality factor was found to decrease by around 30%, from 3.4 and 4.2×10^5, to 0.72 and 1.07×10^5 respectively for the two resonators measured. This decrease is consistent with an increase in the density of TLS due to increased amorphisation of the sapphire substrate by the Ne FIB. Crucially the internal quality factor for the nanowire-embedded resonators is still a factor of 10–100 times greater than other comparable devices. This result therefore indicates that Ne FIB is a promising route towards creating superconducting-nanowire-based devices with low levels of decoherence. A further study of dielectric loss in such devices is warranted and the capabilities of the Ne FIB for creating nanowires with smaller dimensions should also be investigated.

References

[1] E. Levenson-Falk, R. Vijay, and I. Siddiqi, "Nonlinear microwave response of aluminum weak-link josephson oscillators," *Applied Physics Letters*, vol. 98, no. 12, p. 3115, 2011.

[2] A. Blois, S. Rozhko, L. Hao, J. Gallop, and E. Romans, "Proximity effect bilayer nano superconducting quantum interference devices for millikelvin magnetometry," *Journal of Applied Physics*, vol. 114, no. 23, p. 233907, 2013.

[3] O. Astafiev, L. Ioffe, S. Kafanov, Y. A. Pashkin, K. Y. Arutyunov, D. Shahar, O. Cohen, and J. Tsai, "Coherent quantum phase slip," *Nature*, vol. 484, no. 7394, pp. 355–358, 2012.

[4] C. Webster, J. Fenton, T. Hongisto, S. Giblin, A. Zorin, and P. Warburton, "Nbsi nanowire quantum phase-slip circuits: dc supercurrent blockade, microwave measurements, and thermal analysis," *Physical Review B*, vol. 87, no. 14, p. 144510, 2013.

[5] J. Burnett, L. Faoro, I. Wisby, V. Gurtovoi, A. Chernykh, G. Mikhailov, V. Tulin, R. Shaikhaidarov, V. Antonov, P. Meeson, *et al.*, "Evidence for interacting two-level systems from the 1/f noise of a superconducting resonator," *Nature Communications*, vol. 5, 2014.

[6] A. Bruno, G. de Lange, S. Asaad, K. van der Enden, N. Langford, and L. DiCarlo, "Reducing intrinsic loss in superconducting resonators by surface treatment and deep etching of silicon substrates," *Applied Physics Letters*, vol. 106, no. 18, p. 182601, 2015.

[7] S. E. de Graaf, J. Leppäkangas, A. Adamyan, A. Danilov, T. Lindström, M. Fogelström, T. Bauch, G. Johansson, and S. Kubatkin, "Charge qubit coupled to an intense microwave electromagnetic field in a superconducting nb device: Evidence for photon-assisted quasiparticle tunneling," *Physical Review Letters*, vol. 111, no. 13, p. 137002, 2013.

[8] A. Belkin, M. Brenner, T. Aref, J. Ku, and A. Bezryadin, "Little–parks oscillations at low temperatures: Gigahertz resonator method," *Applied Physics Letters*, vol. 98, no. 24, p. 242504, 2011.

[9] M. D. Jenkins, U. Naether, M. Ciria, J. Sesé, J. Atkinson, C. Sánchez-Azqueta, E. del Barco, J. Majer, D. Zueco, and F. Luis, "Nanoscale constrictions in superconducting coplanar waveguide resonators," *Applied Physics Letters*, vol. 105, no. 16, p. 162601, 2014.

[10] J. Peltonen, O. Astafiev, Y. P. Korneeva, B. Voronov, A. Korneev, I. Charaev, A. Semenov, G. Golt'sman, L. Ioffe, T. Klapwijk, *et al.*, "Coherent flux tunneling through nbn nanowires," *Physical Review B*, vol. 88, no. 22, p. 220506, 2013.
[11] H. Wu, D. Ferranti, and L. Stern, "Precise nanofabrication with multiple ion beams for advanced circuit edit," *Microelectronics Reliability*, vol. 54, no. 9, pp. 1779–1784, 2014.
[12] G. Hlawacek, V. Veligura, R. van Gastel, and B. Poelsema, "Helium ion microscopy," *Journal of Vacuum Science & Technology B*, vol. 32, no. 2, p. 020801, 2014.
[13] L. Hao, D. Cox, and J. Gallop, "Characteristics of focused ion beam nanoscale josephson devices," *Superconductor Science and Technology*, vol. 22, no. 6, p. 064011, 2009.
[14] J. Burnett, T. Lindström, M. Oxborrow, Y. Harada, Y. Sekine, P. Meeson, and A. Y. Tzalenchuk, "Slow noise processes in superconducting resonators," *Physical Review B*, vol. 87, no. 14, p. 140501, 2013.
[15] I. Wisby, S. E. de Graaf, R. Gwilliam, A. Adamyan, S. Kubatkin, P. Meeson, A. Y. Tzalenchuk, and T. Lindström, "Coupling of a locally implanted rare-earth ion ensemble to a superconducting microresonator," *Applied Physics Letters*, vol. 105, no. 10, p. 102601, 2014.
[16] S. Probst, F. Song, P. Bushev, A. Ustinov, and M. Weides, "Efficient and robust analysis of complex scattering data under noise in microwave resonators," *Review of Scientific Instruments*, vol. 86, no. 2, p. 024706, 2015.
[17] R. Barends, J. Baselmans, J. Hovenier, J. Gao, S. Yates, T. Klapwijk, and H. Hoevers, "Niobium and tantalum high q resonators for photon detectors," *Applied Superconductivity, IEEE Transactions on*, vol. 17, no. 2, pp. 263–266, 2007.
[18] D. M. Pozar, *Microwave engineering*. John Wiley & Sons, 2009.
[19] J. Zmuidzinas, "Superconducting microresonators: Physics and applications," *Annu. Rev. Condens. Matter Phys.*, vol. 3, no. 1, pp. 169–214, 2012.
[20] N. Constantino, M. Urdampilleta, C. Nash, J. Burnett, J. Morton, J. Fenton, and P. Warburton In preparation, 2015.
[21] R. Janssen, J. Baselmans, A. Endo, L. Ferrari, S. Yates, A. Baryshev, and T. Klapwijk, "High optical efficiency and photon noise limited sensitivity of microwave kinetic inductance detectors using phase readout," *Applied Physics Letters*, vol. 103, no. 20, p. 203503, 2013.
[22] R. Timilsina, S. Tan, R. Livengood, and P. Rack, "Monte carlo simulations of nanoscale focused neon ion beam sputtering of copper: elucidating resolution limits and sub-surface damage," *Nanotechnology*, vol. 25, no. 48, p. 485704, 2014.
[23] J. M. Martinis, K. Cooper, R. McDermott, M. Steffen, M. Ansmann, K. Osborn, K. Cicak, S. Oh, D. Pappas, R. Simmonds, *et al.*, "Decoherence in josephson qubits from dielectric loss," *Physical Review Letters*, vol. 95, no. 21, p. 210503, 2005.